

https://doi.org/10.1070/QEL17976

Line shape and light shift of coherent population trapping resonance under Ramsey interrogation in 'hot' atoms in an optically dense medium

G.V. Voloshin, K.A. Barantsev, A.N. Litvinov

Abstract. **A theory is developed for the effect of coherent population trapping (CPT) in 'hot' atoms under pulsed pumping in an optically dense medium with a buffer gas. The case is considered when the excited level is not degenerate. Based on an analysis of the shape of Ramsey resonances, we show that with increasing optical density of the medium, the dependence of the light shifts of the CPT resonance becomes more and more nontrivial. The dependence of the light shifts of the CPT resonance on the magnitude of the hyperfine splitting of the excited level, concentration of active atoms, temperature, and duration of the dark pause is constructed.**

Keywords: *coherent population trapping, Ramsey method, optically dense medium, 'hot' atoms.*

1. Introduction

It is known that the interaction of bichromatic laser radiation with atomic ensembles leads under certain conditions to the appearance of coherent population trapping (CPT) [1–4]. This phenomenon is resonant in relation to the frequency difference of the incident fields. It is noteworthy that the width of such resonances can be many times (several orders of magnitude) smaller than the natural width of the optical transition. This fact makes it possible to use the CPT phenomenon in various practical applications: in optical magnetometers [5–7], in inversionless lasers [8, 9], in ultrahigh-resolution spectroscopy [10, 11], in devices for recording and processing quantum information [12–14], and in quantum frequency standards [15–22].

One of the possible scenarios for increasing the stability of CPT-based miniature quantum frequency standards is the use of pulsed pumping (Ramsey method) [23, 24]. The essence of this method is as follows: The first long (pumping) pulse transfers the system to a stationary CPT state; then there is a dark pause, during which the system freely evolves, followed by a second short (interrogation) pulse, which detects the system in the CPT state. In this case, the width of Ramsey resonances is determined only by the duration of the dark pause and can reach hundreds or even tens of hertz [24].

In the last decade, many papers have appeared on the study of the shape of CPT resonances with the Ramsey method of pulsed excitation. For example, works [25, 26] are devoted to the study of new methods for increasing the contrast of the CPT resonance. The search for the possibility of increasing the stability of atomic clocks is described in [27–30]. The effect of the buffer gas pressure on the shape of the CPT resonance in the Raman–Ramsey scheme for ^{87}Rb atoms was studied in Refs [31–35], and new methods were tested in Refs [36–38] in order to reduce the light shift of the CPT resonance under pulsed excitation. Lenci et al. [39] observed Ramsey fringes in the study of the effect of light-induced transparency. Liu et al. [40] examined pulsed excitation of the CPT resonance in a closed delta scheme. The methods of suppressing the light shift in Ramsey spectroscopy are discussed in theoretical works [41–45], and experimental verification of these methods was performed in [46, 47].

In the process of creating a frequency standard, it is necessary to increase the signal, which can be done by increasing the number of active atoms. When their concentration n_a reaches a certain value, the effects associated with the absorption of transmitted radiation through a medium with active atoms begin to appear. In this case, the medium is treated to be optically dense. The effect of the optical density of a medium on the shape of the lines of CPT resonances detected by the Ramsey method was considered theoretically in Refs [35, 48, 49]. An increase in the concentration of active atoms is achieved by increasing the temperature of the medium. However, the motion of atoms leads to such effects as Doppler and collisional broadening and level shifts, which in turn results in a decrease in the cross section for light scattering by individual atoms and, as a consequence, in a decrease in the optical thickness of the ensemble. In this regard, the correct account for the influence of the motion of atoms and, consequently, of temperature is a very important problem in the case of optically dense media. Of particular practical interest is the analysis of the effect of the motion of atoms on the frequency shifts of the reference resonances. In this case, random changes in temperature will lead to random changes in these shifts and negatively affect the stability of the CPT-based frequency standard.

The aim of this work is to construct a theory describing the processes of interaction of two-frequency laser radiation with an optically dense medium of alkali atoms, taking into account their temperature. An analysis is performed of changes in the shape and shifts of CPT resonances detected by the Ramsey method, which arise as a result of this interaction, with increasing temperature. It should be noted that, in contrast to Ref. [50], we consider an optically dense medium. This leads to the fact that the task becomes much more time consuming and a number of computational difficulties arise. The main result of this work is the discovery of nonmonotonic

G.V. Voloshin, K.A. Barantsev, A.N. Litvinov Peter the Great St. Petersburg Polytechnic University, ul. Politekhnicheskaya 29, 195251 St. Petersburg, Russia; e-mail: gavriilvsh@gmail.com, kostmann@yandex.ru, andrey.litvinov@mail.ru

Received 19 October 2021; revision received 22 December 2021
Kvantovaya Elektronika **52** (2) 108–115 (2022)
Translated by I.A. Ulitkin

dependences of the light shifts of the CPT resonance under pulsed excitation in an optically dense medium. In Section 2, the mathematical model is described in detail and the basic equations are derived, Section 3 is devoted to the results of numerical calculations. In Section 4, the main conclusions of the work are formulated.

2. Mathematical model

To construct a mathematical model of the interaction of bichromatic laser radiation with an atomic medium, we will use a semi-classical approach, in which radiation is described as a plane electromagnetic wave with two carrier frequencies (ω_1 and ω_2) propagating along the z axis. The vector of the electric component intensity of such a wave can be written in the form

$$\boldsymbol{E}(z,t) = \boldsymbol{E}_1(z,t)\exp[-\mathrm{i}(\omega_1 t - k_1 z)] + \boldsymbol{E}_2(z,t)\exp[-\mathrm{i}(\omega_2 t - k_2 z)] + \text{c.c.}, \quad (1)$$

where k_j and E_j are the wavenumbers and complex amplitudes of the corresponding frequency components of the wave ($j = 1, 2$).

The field of such a wave contains a medium of active alkali atoms and a buffer gas. Let us consider a four-level atomic model (Fig. 1), in which the first two states $|g\rangle$, $g = 1, 2$ are assumed to be ground states corresponding to the hyperfine splitting of the s-state, and the other two states $|e\rangle$, $e = 3, 4$ are the excited states corresponding to hyperfine splitting of the p-state. In this case, the frequencies of the fields $\boldsymbol{E}_1$ and $\boldsymbol{E}_2$ will be considered close to the frequencies of the transitions $|1\rangle \leftrightarrow |e\rangle$ and $|2\rangle \leftrightarrow |e\rangle$.

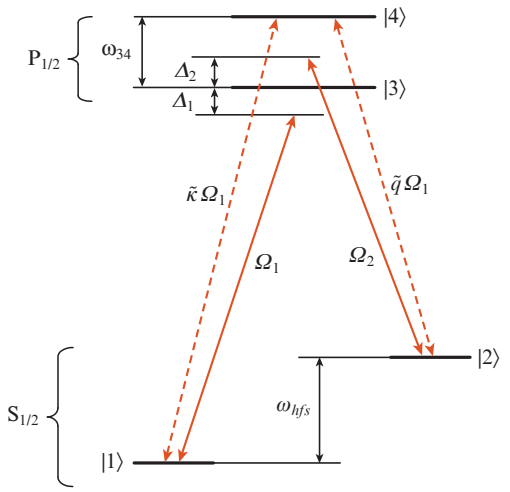

Figure 1. Diagram of energy levels of active atoms and excited transitions.

The state of an ensemble of active atoms will be described by the method of a one-particle density matrix, which in Wigner's representation in terms of the translational degrees of freedom of atoms $[(\hat{\rho}(\boldsymbol{p},\boldsymbol{r},t))]$ satisfies the quantum kinetic equation [51]:

$$\left(\frac{\partial}{\partial t} + \frac{\boldsymbol{p}}{m}\nabla\right)\hat{\rho}(\boldsymbol{p},\boldsymbol{r},t) = -\frac{\mathrm{i}}{\hbar}[\hat{H},\hat{\rho}(\boldsymbol{p},\boldsymbol{r},t)] + \hat{\hat{R}}\{\hat{\rho}(\boldsymbol{p},\boldsymbol{r},t)\} + \hat{\hat{S}}\{\hat{\rho}(\boldsymbol{p},\boldsymbol{r},t)\}, \quad (2)$$

where m is the mass of the atom; $\boldsymbol{p} = m\boldsymbol{v}$ is the momentum of the translational motion of the atom; $\hat{H}$ is the Hamiltonian of the system; $\hat{\hat{R}}$ is the operator that phenomenologically takes into account the spontaneous relaxation of atoms; and $\hat{\hat{S}}$ is the operator of collision integrals. Collisions are assumed to be both between active atoms and buffer gas atoms.

The Hamiltonian of an atom can be represented as $\hat{H} = \hat{H}_0 + \hat{V}$, where

$$\hat{H}_0 = \sum_{n=1}^{4} |n\rangle\langle n|$$

is the Hamiltonian of an atom that does not interact with the field;

$$\hat{V} = -\hat{\boldsymbol{d}}\boldsymbol{E}(\boldsymbol{r},t) = -d_{31}(E_1\exp[-\mathrm{i}(\omega_1 t - k_1 z)] + E_1^*\exp[\mathrm{i}(\omega_1 t - k_1 z)])|3\rangle\langle 1| - d_{32}(E_2\exp[-\mathrm{i}(\omega_2 t - k_2 z)] + E_2^*\exp[\mathrm{i}(\omega_2 t - k_2 z)])|3\rangle\langle 2| - d_{41}(E_1\exp[-\mathrm{i}(\omega_1 t - k_1 z)] + E_1^*\exp[\mathrm{i}(\omega_1 t - k_1 z)])|4\rangle\langle 1| - d_{42}(E_2\exp[-\mathrm{i}(\omega_2 t - k_2 z)] + E_2^*\exp[\mathrm{i}(\omega_2 t - k_2 z)])|4\rangle\langle 2| + \text{h.c.} \quad (3)$$

is the operator of interaction in the dipole approximation; $\hat{\boldsymbol{d}} = \boldsymbol{e}_\mathrm{d}\hat{d}$ is the operator of the dipole moment of the atom; and $d_{nm} = \langle n|\hat{d}|m\rangle$ are its matrix elements. In expression (3), we neglected the terms $\sim d_{ge}E_{g'}$ for $g \neq g'$, $e = 3, 4$, assuming that the field E_1 is significantly detuned from the transitions $|2\rangle \leftrightarrow |e\rangle$, and the field E_2, from the transitions $|1\rangle \leftrightarrow |e\rangle$. We also neglect the effects associated with the vector nature of the field. We assume that the vector of the dipole moment of the atom is codirectional with the polarisation vectors of the wave ($\boldsymbol{e}_\mathrm{d}\boldsymbol{e}_j = 1$, $\boldsymbol{e}_j = \boldsymbol{E}_j/E_j$, $j = 1, 2$). The matrix element $d_{12} = 0$, since the electric dipole transition $|1\rangle \leftrightarrow |2\rangle$ is forbidden.

We emphasise that in the theoretical analysis of CPT effects, a simple three-level Λ-scheme of atomic states is very often used. At the same time, it is well known that the multilevel nature of real atoms can significantly affect the optical properties of atomic ensembles and, in particular, the CPT and electromagnetically induced transparency effects [52–55]. In this case, it turns out [49, 50, 56] that taking into account even one additional excited state in the theoretical description leads to significant differences from the predictions obtained in the description of CPT in the framework of the Λ-model. Therefore, in this work, we analyse the simplest case of a multilevel system, namely, we take into account the presence of two excited states.

By assuming that the wave front is plane, the field diffraction is small at the cell edges, and the optical properties of the ensemble are uniform, we will neglect the dependence of the density matrix on the coordinates in the directions transverse to the laser beam, $\hat{\rho} = \hat{\rho}(\boldsymbol{v},z,t)$.

We write the elements of the collision integrals matrix in the strong collision model:

$$\left(\hat{\hat{S}}\{\hat{\rho}(\boldsymbol{v},z,t)\}\right)_{jj} = -\nu\rho_{jj}(\boldsymbol{v},z,t) + \sum_{\substack{n=1 \\ (n,j)\neq(g,e)}}^{4} \nu_{nj}M(\boldsymbol{v})\int\rho_{nn}(\boldsymbol{v}',z,t)\,\mathrm{d}\boldsymbol{v}', \quad j = \overline{1,4}, \quad (4)$$

$$\left(\hat{\hat{S}}\{\hat{\rho}(\boldsymbol{v},z,t)\}\right)_{12} = \left(\hat{\hat{S}}\{\hat{\rho}(\boldsymbol{v},z,t)\}\right)^*_{21}$$

$$= -\nu\rho_{12}(\boldsymbol{v},z,t) + \nu_{\text{coh}}^{vv'} M(\boldsymbol{v}) \int \rho_{12}(\boldsymbol{v}',z,t)\,\mathrm{d}\boldsymbol{v}', \quad (5)$$

$$\left(\hat{\hat{S}}\{\hat{\rho}(\boldsymbol{v},z,t)\}\right)_{ge} = \left(\hat{\hat{S}}\{\hat{\rho}(\boldsymbol{v},z,t)\}\right)^*_{eg} = -\nu\rho_{ge}(\boldsymbol{v},z,t), \quad (6)$$

$$g = 1,2,\ e = 3,4,$$

where $M(\boldsymbol{v}) = (\sqrt{\pi}\,v_T)^{-3}\exp(-\boldsymbol{v}^2/v_T^2)$ is the Maxwellian velocity distribution; $v_T = \sqrt{2k_{\text{B}}T/m}$ is the most probable speed of translational motion of atoms; ν is the total collision frequency; ν_{nm} is the collision frequency leading to transitions from state $|n\rangle$ to state $|m\rangle$; and $\nu_{nm}^{vv'}$ is the frequency of collisions at which the low-frequency coherence $\rho_{12}(\boldsymbol{v},z,t)$ is preserved. It is assumed here that the energy of the thermal motion of atoms is insufficient for their excitation, as a result of which the corresponding terms 'inputted' to the given velocity group are excluded from the summation in (4). Also here we restrict ourselves to the approximation in which the optical coherences $\rho_{ge}(\boldsymbol{v},z,t)$ are destroyed in any collision, due to which the 'input' terms in (6) are completely absent.

In all off-diagonal elements of the density matrix, a substitution is made that selects a rapidly oscillating factor:

$$\rho_{ge}(\boldsymbol{v},z,t) = \rho^*_{eg}(\boldsymbol{v},z,t) = \exp[\mathrm{i}(\omega_g t - k_g z)]\tilde{\rho}_{ge}(\boldsymbol{v},z,t), \quad (7)$$

$$g = 1,2,\ e = 3,4,$$

$$\rho_{12}(\boldsymbol{v},z,t) = \rho^*_{21}(\boldsymbol{v},z,t)$$

$$= \exp[\mathrm{i}(\omega_1 - \omega_2)t - \mathrm{i}(k_1 - k_2)z]\tilde{\rho}_{12}(\boldsymbol{v},z,t). \quad (8)$$

The terms arising after substituting (7), (8) into (2) and oscillating with a double frequency ($\sim\exp[\pm 2\mathrm{i}(\omega_g t - k_g z)]$), will be discarded in the framework of the rotating wave approximation. Then the element-wise derived equation (2) has the form:

$$\dot{\rho}_{11}(\boldsymbol{v}) + \boldsymbol{v}\nabla\rho_{11}(\boldsymbol{v}) = -\mathrm{i}\Omega_1\tilde{\rho}_{13}(\boldsymbol{v}) + \mathrm{i}\Omega_1^*\tilde{\rho}_{31}(\boldsymbol{v}) - \mathrm{i}\tilde{\kappa}\Omega_1^*\tilde{\rho}_{14}(\boldsymbol{v})$$
$$+ \mathrm{i}\tilde{\kappa}^*\Omega_1^*\tilde{\rho}_{41}(\boldsymbol{v}) + \frac{\gamma}{2}(\rho_{33}(\boldsymbol{v}) + \tilde{\kappa}^2\rho_{44}(\boldsymbol{v})) - \nu\rho_{11}(\boldsymbol{v})$$
$$+ \nu_{11}M(\boldsymbol{v})\int\rho_{11}(\boldsymbol{v}')\,\mathrm{d}\boldsymbol{v}' + \nu_{21}M(\boldsymbol{v})\int\rho_{22}(\boldsymbol{v}')\,\mathrm{d}\boldsymbol{v}'$$
$$+ \nu_{31}M(\boldsymbol{v})\int\rho_{33}(\boldsymbol{v}')\,\mathrm{d}\boldsymbol{v}' + \nu_{41}M(\boldsymbol{v})\int\rho_{44}(\boldsymbol{v}')\,\mathrm{d}\boldsymbol{v}', \quad (9)$$

$$\dot{\rho}_{22}(\boldsymbol{v}) + \boldsymbol{v}\nabla\rho_{22}(\boldsymbol{v}) = -\mathrm{i}\Omega_2\tilde{\rho}_{23}(\boldsymbol{v}) + \mathrm{i}\Omega_2^*\tilde{\rho}_{32}(\boldsymbol{v})$$
$$- \mathrm{i}\tilde{q}\Omega_2\tilde{\rho}_{24}(\boldsymbol{v}) + \mathrm{i}\tilde{q}^*\Omega_2^*\tilde{\rho}_{42}(\boldsymbol{v}) + \frac{\gamma}{2}(\rho_{33}(\boldsymbol{v}) + \tilde{q}^2\rho_{44}(\boldsymbol{v}))$$
$$- \nu\rho_{22}(\boldsymbol{v}) + \nu_{22}M(\boldsymbol{v})\int\rho_{22}(\boldsymbol{v}')\,\mathrm{d}\boldsymbol{v}' + \nu_{12}M(\boldsymbol{v})\int\rho_{11}(\boldsymbol{v}')\,\mathrm{d}\boldsymbol{v}'$$
$$+ \nu_{32}M(\boldsymbol{v})\int\rho_{33}(\boldsymbol{v}')\,\mathrm{d}\boldsymbol{v}' + \nu_{42}M(\boldsymbol{v})\int\rho_{44}(\boldsymbol{v}')\,\mathrm{d}\boldsymbol{v}', \quad (10)$$

$$\dot{\rho}_{33}(\boldsymbol{v}) + \boldsymbol{v}\nabla\rho_{33}(\boldsymbol{v}) = \mathrm{i}\Omega_1\tilde{\rho}_{13}(\boldsymbol{v}) - \mathrm{i}\Omega_1^*\tilde{\rho}_{31}(\boldsymbol{v}) + \mathrm{i}\Omega_2\tilde{\rho}_{23}(\boldsymbol{v})$$
$$- \mathrm{i}\Omega_2^*\tilde{\rho}_{32}(\boldsymbol{v}) - \gamma\rho_{33}(\boldsymbol{v}) - \nu\rho_{33}(\boldsymbol{v})$$
$$+ \nu_{33}M(\boldsymbol{v})\int\rho_{33}(\boldsymbol{v}')\,\mathrm{d}\boldsymbol{v}' + \nu_{43}M(\boldsymbol{v})\int\rho_{44}(\boldsymbol{v}')\,\mathrm{d}\boldsymbol{v}', \quad (11)$$

$$\dot{\rho}_{44}(\boldsymbol{v}) + \boldsymbol{v}\nabla\rho_{44}(\boldsymbol{v}) = \mathrm{i}\tilde{\kappa}\Omega_1\tilde{\rho}_{14}(\boldsymbol{v}) - \mathrm{i}\tilde{\kappa}^*\Omega_1^*\tilde{\rho}_{41}(\boldsymbol{v})$$
$$+ \mathrm{i}\tilde{q}\Omega_2\tilde{\rho}_{24}(\boldsymbol{v}) - \mathrm{i}\tilde{q}^*\Omega_2^*\tilde{\rho}_{42}(\boldsymbol{v}) - \frac{\gamma}{2}(\tilde{\kappa}^2 + \tilde{q}^2)\rho_{44}(\boldsymbol{v}) - \nu\rho_{44}(\boldsymbol{v})$$
$$+ \nu_{44}M(\boldsymbol{v})\int\rho_{44}(\boldsymbol{v}')\,\mathrm{d}\boldsymbol{v}' + \nu_{34}M(\boldsymbol{v})\int\rho_{33}(\boldsymbol{v}')\,\mathrm{d}\boldsymbol{v}', \quad (12)$$

$$\dot{\tilde{\rho}}_{12}(\boldsymbol{v}) + \boldsymbol{v}\nabla\tilde{\rho}_{12}(\boldsymbol{v}) = \mathrm{i}\Omega_1^*\tilde{\rho}_{32}(\boldsymbol{v}) - \mathrm{i}\Omega_2\tilde{\rho}_{13}(\boldsymbol{v}) + \mathrm{i}\tilde{\kappa}^*\Omega_1^*\tilde{\rho}_{42}(\boldsymbol{v})$$
$$- \mathrm{i}\tilde{q}\Omega_2\tilde{\rho}_{14}(\boldsymbol{v}) + [\mathrm{i}((\Delta_2 - \Delta_1) + (k_1 - k_2)\boldsymbol{v}) - \Gamma_{12} - \nu]\tilde{\rho}_{12}(\boldsymbol{v})$$
$$+ \nu_{\text{coh}}^{vv'} M(\boldsymbol{v})\int\tilde{\rho}_{12}(\boldsymbol{v}')\,\mathrm{d}\boldsymbol{v}', \quad (13)$$

$$\dot{\tilde{\rho}}_{13}(\boldsymbol{v}) + \boldsymbol{v}\nabla\tilde{\rho}_{13}(\boldsymbol{v}) = -\mathrm{i}\Omega_1^*\tilde{\rho}_{11}(\boldsymbol{v}) - \mathrm{i}\Omega_2^*\tilde{\rho}_{12}(\boldsymbol{v}) + \mathrm{i}\Omega_1^*\tilde{\rho}_{33}(\boldsymbol{v})$$
$$+ [-\mathrm{i}(\Delta_1 - k_1 v) - \Gamma - \nu]\tilde{\rho}_{13}(\boldsymbol{v}), \quad (14)$$

$$\dot{\tilde{\rho}}_{14}(\boldsymbol{v}) + \boldsymbol{v}\nabla\tilde{\rho}_{14}(\boldsymbol{v}) = -\mathrm{i}\tilde{\kappa}^*\Omega_1^*\tilde{\rho}_{11}(\boldsymbol{v}) - \mathrm{i}\tilde{q}^*\Omega_2^*\tilde{\rho}_{12}(\boldsymbol{v})$$
$$+ \mathrm{i}\tilde{\kappa}^*\Omega_1^*\tilde{\rho}_{44}(\boldsymbol{v}) + [-\mathrm{i}(\Delta_1 - \omega_{34} - k_1 v) - \Gamma - \nu]\tilde{\rho}_{14}(\boldsymbol{v}), \quad (15)$$

$$\dot{\tilde{\rho}}_{23}(\boldsymbol{v}) + \boldsymbol{v}\nabla\tilde{\rho}_{23}(\boldsymbol{v}) = -\mathrm{i}\Omega_1^*\tilde{\rho}_{21}(\boldsymbol{v}) - \mathrm{i}\Omega_2^*\rho_{22}(\boldsymbol{v})$$
$$+ \mathrm{i}\Omega_2^*\rho_{33}(\boldsymbol{v}) + [-\mathrm{i}(\Delta_2 - k_2 v) - \Gamma - \nu]\tilde{\rho}_{23}(\boldsymbol{v}), \quad (16)$$

$$\dot{\tilde{\rho}}_{24}(\boldsymbol{v}) + \boldsymbol{v}\nabla\tilde{\rho}_{24}(\boldsymbol{v}) = -\mathrm{i}\tilde{\kappa}^*\Omega_1^*\tilde{\rho}_{21}(\boldsymbol{v}) - \mathrm{i}\tilde{q}^*\Omega_2^*\tilde{\rho}_{22}(\boldsymbol{v})$$
$$+ \mathrm{i}\tilde{q}^*\Omega_2^*\tilde{\rho}_{44}(\boldsymbol{v}) + [-\mathrm{i}(\Delta_2 - \omega_{34} - k_2 v) - \Gamma - \nu]\tilde{\rho}_{24}(\boldsymbol{v}), \quad (17)$$

where $\Omega_g = d_{3g}E_g/\hbar$ are the Rabi frequencies of the corresponding fields; $\tilde{\kappa} = d_{41}/d_{31}$ and $\tilde{q} = d_{42}/d_{32}$ are the ratios of the matrix elements of the dipole moment operator; $\Delta_g = \omega_g - \omega_{g3}^{\text{at}}$ are field detunings from atomic transitions $|g\rangle \leftrightarrow |3\rangle$; γ is the rate of decay of the excited state $|3\rangle$; Γ and Γ_{12} are the decay rates of optical and low-frequency coherences, respectively; and v is the projection of the velocity vector $\boldsymbol{v}$ onto the z axis. Here, we use the weak field approximation ($\Omega_g \ll \nu$), which allows one to neglect the populations of excited states in comparison with the populations of the ground states ($\rho_{ee} \ll \rho_{gg}$). The arguments z and t have been omitted for brevity.

Note that the system of equations (9)–(17) was written without taking into account the long-range dipole-dipole interatomic interaction [57, 58], which is associated with the weakening of the resonance nature of this interaction in ensembles of atoms heated to high temperatures [59–61]. In this case, we will take into account the collective polyatomic effects due to the finite optical thickness [see below (32)].

To simplify this system, we pass to the reduced density matrix $\rho_{nm}(z,t) = \int\rho_{nm}(\boldsymbol{v},z,t)\mathrm{d}\boldsymbol{v}$ by integrating equations (9)–(13) over the velocities. In this case, due to the mentioned weak-field approximation, the rate dependences of the populations of the ground states and low-frequency coherence can be considered Maxwellian:

$$\rho_{gg}(\boldsymbol{v},z,t) = M(\boldsymbol{v})\rho_{gg}(z,t), \quad (18)$$

$$\tilde{\rho}_{12}(\boldsymbol{v},z,t) = M(\boldsymbol{v})\tilde{\rho}_{12}(z,t). \quad (19)$$

The terms proportional to the gradients in the left-hand sides of Eqns (9)–(13) are discarded, neglecting the edge effects. Then equations (9)–(13) after integration over velocities take the form:

$$\dot{\rho}_{11} = -2\,\mathrm{Re}\{\mathrm{i}\Omega_1[\tilde{\rho}_{13} + \tilde{\kappa}\tilde{\rho}_{14}]\} + \frac{\gamma}{2}(\rho_{33} + \tilde{\kappa}^2\rho_{44}) + (\nu_{11} - \nu)\rho_{11} + \nu_{21}\rho_{22} + \nu_{31}\rho_{33} + \nu_{41}\rho_{44}, \quad (20)$$

$$\dot{\rho}_{22} = -2\,\mathrm{Re}\{\mathrm{i}\Omega_2[\tilde{\rho}_{23} + \tilde{\kappa}\tilde{\rho}_{14}]\} + \frac{\gamma}{2}(\rho_{33} + \tilde{q}^2\rho_{44}) + (\nu_{22} - \nu)\rho_{22} + \nu_{12}\rho_{11} + \nu_{32}\rho_{33} + \nu_{42}\rho_{44}, \quad (21)$$

$$\dot{\rho}_{33} = 2\,\mathrm{Re}\{\mathrm{i}[\Omega_1\tilde{\rho}_{13} + \Omega_2\tilde{\rho}_{23}]\} - \gamma'\rho_{33} + \nu_{43}\rho_{44}, \quad (22)$$

$$\dot{\rho}_{44} = 2\,\mathrm{Re}\{\mathrm{i}[\Omega_1\tilde{\kappa}\tilde{\rho}_{14} + \Omega_2\tilde{q}\tilde{\rho}_{24}]\} - \frac{\gamma}{2}(\tilde{\kappa}^2 + \tilde{q}^2)\rho_{44} + (\nu - \nu_{44})\rho_{44} + \nu_{34}\rho_{33}, \quad (23)$$

$$\dot{\tilde{\rho}}_{12} = \mathrm{i}[\Omega_1^*\tilde{\rho}_{32} - \Omega_2\tilde{\rho}_{13} + \tilde{\kappa}^*\Omega_1^*\tilde{\rho}_{42} - \tilde{q}\Omega_2\tilde{\rho}_{14}] + [\mathrm{i}\delta - \Gamma'_{12}]\tilde{\rho}_{12}, \quad (24)$$

where $\gamma' = \gamma + \nu - \nu_{33}$; $\Gamma'_{12} = \Gamma_{12} + \nu - \nu_{\mathrm{coh}}^{\nu\nu'}$; $\Gamma' = \Gamma + \nu$ are decay rates modified due to collisions; and $\delta = \Delta_2 - \Delta_1$ is the two-photon detuning. The arguments z and t are omitted.

The change in the optical coherences along the coordinate can be neglected, since they are destroyed in each collision, and the mean free path of atoms is assumed to be much shorter than the ensemble length. Thus, the gradients in equations (14)–(17) also vanish.

Due to the presence of terms $\sim k_g v$, which take into account the Doppler frequency shift, the transition to the reduced elements by integrating equations (14)–(17) is impossible. In this regard, the optical coherences from these equations are first expressed in terms of quadratures by the method of undefined coefficients and only then are they integrated over the velocities:

$$\tilde{\rho}_{g3}(t) = -\mathrm{i}\int_0^t \mathrm{d}t'[\Omega_2^*(t')\tilde{\rho}_{g2}(t') + \Omega_1^*(t')\tilde{\rho}_{g1}(t')] \times \int_{-\infty}^{\infty} \mathrm{d}\boldsymbol{v} M(\boldsymbol{v}) \exp[-(\mathrm{i}(\Delta_g - k_g v) + \Gamma')(t - t')], \quad (25)$$

$$\tilde{\rho}_{g4}(t) = -\mathrm{i}\int_0^t \mathrm{d}t'[\tilde{q}^*\Omega_2^*(t')\tilde{\rho}_{g2}(t') + \tilde{\kappa}^*\Omega_1^*(t')\tilde{\rho}_{g1}(t')] \times \int_{-\infty}^{\infty} \mathrm{d}\boldsymbol{v} M(\boldsymbol{v}) \exp[-(\mathrm{i}(\Delta_g - \omega_{34} - k_g v) + \Gamma')(t - t')]. \quad (26)$$

The argument z will be omitted hereinafter. The dynamics of the system is considered from the moment $t = 0$, when the optical coherences are equal to zero, which determines the choice of the lower limit of integration over time.

The resulting velocity integrals are of the Gaussian type and are expressed analytically:

$$\tilde{\rho}_{g3}(t) = -\mathrm{i}\int_0^t \mathrm{d}t' \exp\left[-\frac{v_T^2 k_g^2}{2}(t - t') - (\mathrm{i}\Delta_g + \Gamma')(t - t')\right] \times [\Omega_2^*(t')\tilde{\rho}_{g2}(t') + \Omega_1^*(t')\tilde{\rho}_{g1}(t')], \quad (27)$$

$$\tilde{\rho}_{g4}(t) = -\mathrm{i}\int_0^t \mathrm{d}t' \times \exp\left[-\frac{v_T^2 k_g^2}{4}(t - t')^2 - (\mathrm{i}(\Delta_g - \omega_{34}) + \Gamma')(t - t')\right] \times [\tilde{q}^*\Omega_2^*(t')\tilde{\rho}_{g2}(t') + \tilde{\kappa}^*\Omega_1^*(t')\tilde{\rho}_{g1}(t')]. \quad (28)$$

Substituting (27) and (28) in (20)–(24), we obtain a system of homogeneous Volterra integro-differential equations of the first kind, which allows further numerical solution. However, due to the computational complexity of this system, we will use the following approximation. Since the kernels of the integrals in (27) and (28) are exponents oscillating and decaying with time, by neglecting the change in the sought-for functions at the times of such oscillations [62], we can move them outside the integrals at the time corresponding to the upper limit of integration. Then, after expressing the integrals explicitly, we obtain:

$$\tilde{\rho}_{g3}(t) = \frac{-\mathrm{i}\sqrt{\pi}}{k_j v_T}(\Omega_{20}^*\tilde{\rho}_{g2}(t) + \Omega_{10}^*\tilde{\rho}_{g1}(t)) \times \left\{w\left(\frac{\mathrm{i}\Gamma' - \Delta_g}{k_g v_T}\right) - \exp\left[-\left(\frac{k_g^2 v_T^2}{4}t^2 + (\Gamma' + \Delta_g)t\right)\right] \times w\left(\mathrm{i}\frac{k_g v_T}{2}t + \frac{i\Gamma' - \Delta_g}{k_g v_T}\right)\right\}, \quad (29)$$

$$\tilde{\rho}_{g4}(t) = \frac{-\mathrm{i}\sqrt{\pi}}{k_j v_T}(\tilde{q}^*\Omega_{20}^*\tilde{\rho}_{g2}(t) + \tilde{\kappa}^*\Omega_{10}^*\tilde{\rho}_{g1}(t)) \times \left\{w\left(\frac{\mathrm{i}\Gamma' - (\Delta_g - \omega_{34})}{k_g v_T}\right) - \exp\left[-\left(\frac{k_g^2 v_T^2}{4}t^2 + (\Gamma' + (\Delta_g - \omega_{34}))t\right)\right] w\left(\mathrm{i}\frac{k_g v_T}{2}t + \frac{\mathrm{i}\Gamma' - (\Delta_g - \omega_{34})}{k_g v_T}\right)\right\}, \quad (30)$$

where $w(z) = \exp(-z^2)[1 - \mathrm{erf}(-\mathrm{i}z)]$ is the Faddeeva function; and

$$\mathrm{erf}\, z = \frac{2}{\sqrt{\pi}}\int_0^z \exp(-z^2)\mathrm{d}z$$

is the error function.

After substituting (29), (30) into (20)–(24), we obtain a system of ordinary differential equations of the first order.

To establish the coordinate dependences of the fields, we use the truncated equation for their complex amplitudes in a nonmagnetic isotropic medium with a nonzero vector of macroscopic polarisation $P(z,t)$:

$$\left(\frac{\partial}{\partial z} + \frac{1}{c}\frac{\partial}{\partial t}\right)\{\mathrm{i}k_1 E_1 \exp[-\mathrm{i}(\omega_1 t - k_1 z)] + \mathrm{i}k_2 E_2 \exp[-\mathrm{i}(\omega_2 t - k_2 z)] + \mathrm{c.c.}\} = \frac{2\pi}{c^2}\frac{\partial^2 P}{\partial t^2}. \quad (31)$$

We calculate the macroscopic polarisation of the medium as the quantum-mechanical average of the dipole moment per unit volume

$$P(z,t) = n_a \mathrm{Sp}(\hat{d}\hat{\rho})$$

$$= n_a \sum_{g,e} \tilde{\rho}_{ge}(z,t) d_{eg} \exp[\mathrm{i}(\omega_g t - k_g z)] + \text{c.c.}, \quad (32)$$

where the averaging is performed over the internal degrees of freedom of the atom and over its translational velocity, rather than over its coordinate, since we are interested in the polarisation of the medium in an infinitely small neighbourhood of the point z.

After substituting (32) into (31), assuming slow changes in the amplitudes of the density matrix elements ($\partial\tilde{\rho}_{ge}/\partial z \ll k_g\tilde{\rho}_{ge}$, $\partial\tilde{\rho}_{ge}/\partial t \ll \omega_g\tilde{\rho}_{ge}$), we multiply both sides of the resulting equation sequentially by both complex exponents $\exp[\mathrm{i}(\omega_g t - k_g z)]$ and again use the rotating wave approximation. As a result, we obtain

$$\frac{\partial E_1}{\partial z} + \frac{1}{c}\frac{\partial E_1}{\partial t} = 2\pi \mathrm{i} n_a k_1 d_{31}(\tilde{\rho}_{31} + \tilde{\kappa}\tilde{\rho}_{41}), \quad (33)$$

$$\frac{\partial E_2}{\partial z} + \frac{1}{c}\frac{\partial E_2}{\partial t} = 2\pi \mathrm{i} n_a k_2 d_{32}(\tilde{\rho}_{32} + \tilde{q}\tilde{\rho}_{42}). \quad (34)$$

Let us neglect the changes in the field amplitudes at the times of flight by the photon over the ensemble length, which will allow us to neglect the second terms in the left-hand sides of (33) and (34). We finally write

$$\frac{\partial \Omega_1}{\partial z} = \frac{2\pi \mathrm{i} n_a k_1 |d_{31}|^2}{\hbar}(\tilde{\rho}_{31} + \tilde{\kappa}\tilde{\rho}_{41}), \quad (35)$$

$$\frac{\partial \Omega_2}{\partial z} = \frac{2\pi \mathrm{i} n_a k_2 |d_{32}|^2}{\hbar}(\tilde{\rho}_{32} + \tilde{q}\tilde{\rho}_{42}) \quad (36)$$

in terms of Rabi frequencies

3. Discussion of the results

The consistent solution of equations (20)–(24) after substituting (29) and (30) into them together with (35) and (36) allows one to obtain information both about the evolution of the quantum state of the ensemble along its entire length, and about the change in the field amplitudes as they pass through the medium for arbitrary waveform input laser signals. In our work, we study the features of the behaviour of CPT resonances, which are detected by two rectangular pulses separated in time by a dark pause T_d, as, for example, in Ref. [35].

The first pump pulse has a duration τ_p sufficient to establish a stationary CPT state in the ensemble ($\tau_p \gg \gamma/\Omega_{j0}^2$). The second short pulse of duration τ detects the system in the CPT state.

Let us discuss the results of the numerical solution of the system in question with the given boundary condition. First we analyse the process of field absorption by the medium towards the end of the interrogation pulse.

As can be seen from Fig. 2, the intensities of the fields decrease exponentially with penetration into the medium. The decrease is faster if the temperature of the absorbing medium is higher, since the concentration of the saturated vapour of the active medium in the gas cell increases with increasing temperature. In the considered model, this is taken into account by introducing the given empirical dependence of the concentration of active atoms on temperature [63]:

$$n_a(T) = \quad (37)$$

$$\begin{cases} (1.3\times 10^{-3} k_B T)^{-1} \times 10^{2.881 + 4.857 - 4215/T}, & T < 321.1\,\mathrm{K}, \\ (1.3\times 10^{-3} k_B T)^{-1} \times 10^{2.881 + 4.312 - 4040/T}, & T > 321.1\,\mathrm{K}. \end{cases}$$

It should be noted that this dependence remains valid only in the temperature range from 298 to 550 K.

At any temperature in the range under consideration, the field experiences stronger absorption at a nonzero two-photon detuning (Fig. 2b) rather than at a zero detuning (Fig. 2a), which is a consequence of the coherent trapping of atoms in the ground state.

Let us now see how the intensities change with increasing temperature after passing through the medium at various detunings (Fig. 3).

With an increase in temperature, resonances undergo transition into the region of lower intensities. Due to the absorption effects mentioned above, at high temperatures and detunings outside the reference resonance, the intensity decreases more strongly (Fig. 3a). The amplitude of the reference resonance due to absorption increases up to a temperature $T \approx 45\,^\circ$C, after which absorption leads to its decrease (Fig. 3b).

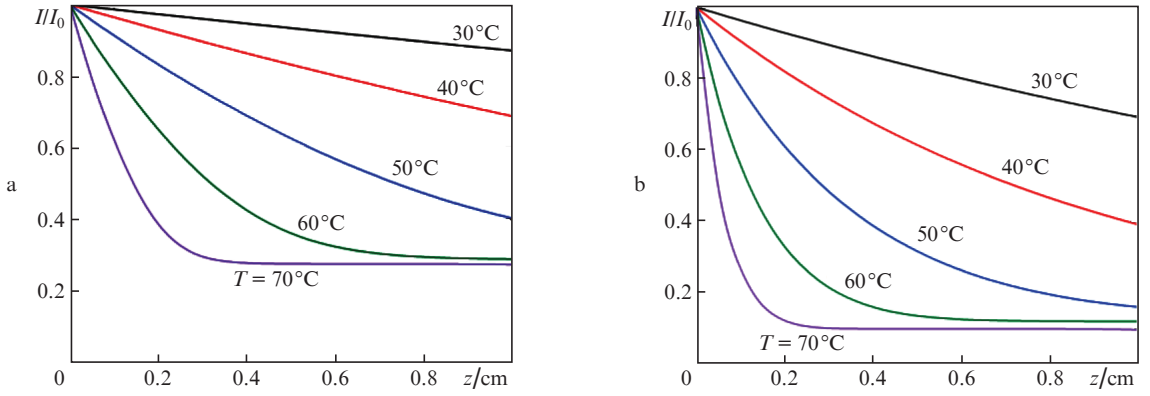

Figure 2. (Colour online) Dependences of the radiation intensity at the end of the interrogation pulse, referred to the field intensity at the entrance to the medium, on the relative penetration depth at different temperatures T for (a) $\delta = 0$ and (b) π/T_d; $m_a = 87$ amu, $m_{buf} = 28$ amu, $n_{buf} = 10^{19}$ cm^{-3}, $\gamma = 10^7$ s^{-1}, $\Gamma = \gamma/4$, $\Gamma_{12} = 100$ s^{-1}, $\Delta_1 = \delta/2$, $\Delta_2 = -\delta/2$, $\eta = 0.01$, $T_d = 5$ ms, $\omega_{34} = 10\gamma$, $\tau = 10\gamma^{-1}$, $\tilde{q} = 0.5$, $\tilde{\kappa} = 1$.

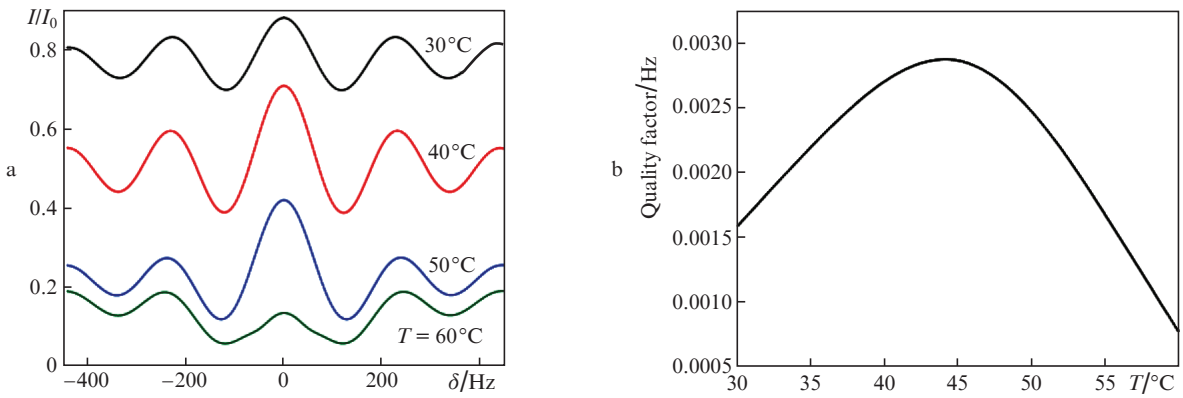

Figure 3. (Colour online) (a) Shapes of CPT resonances, detected by the Ramsey method from the intensity of the output radiation, for different temperatures, as well as (b) dependence of the quality factor of the reference resonance on temperature; the cell length $L = 1$ cm; other parameters are the same as in Fig. 2.

Figure 4a shows the temperature dependences of the shift of the reference resonance maximum S relative to the zero of the two-photon detuning. With increasing temperature, the shift increases in a somewhat nonmonotonic manner. The slowest change occurs in the initial interval from 30 to 45 °C, where the shift decreases. In this case, the dependences of this shift on the frequency of hyperfine splitting of the excited state ω_{34}, as in the case of a thin medium, have the form of a dispersion contour (Fig. 4b). It is noteworthy that at a temperature in the vicinity of $T \approx 55$ °C, the shift changes its sign regardless of the value of ω_{34}. It is also logical that at $\omega_{34} \to 0$ or $\omega_{34} \to \infty$ we have a situation similar to that arising in the Λ-system, and the shift of the CPT of the resonance will be equal in this case to zero. On the contrary, when the excited state is nondegenerate (especially in the region $200\gamma < \omega_{34} < 800\gamma$), we are dealing with a more complicated situation. In this case, the shape of the CPT resonance can become asymmetric [64, 65] and a light shift can occur, which depends on temperature in a nontrivial way.

It can be seen from Fig. 5a that with an increase in the buffer gas concentration n_{buf}, the amplitude of the resonances increases. Thus, the light shift changes in a nonmonotonic manner and reaches its maximum value at $n_{\text{buf}} < 4 \times 10^{18}\text{cm}^{-3}$ (Fig. 5b), and at low concentrations of the buffer gas, the resonance shape becomes more asymmetric. Note that the asymmetry of the shape is possible only for systems with nonunity coefficients $\tilde{\kappa}$ and $\tilde{q}$.

Let us now analyse the effect of external laser radiation parameters on the resonance shape.

With an increase in the Rabi frequencies of external fields, the amplitudes of the resonances increase, and the widths slightly decrease, while being at the same intensity level (Fig. 6a). Thus, by increasing the Rabi frequency of external fields, it is possible to effectively increase the quality factor of resonances in intensity. However, the solution to the problem in question does not allow the behaviour of the system to be analysed in the Rabi frequency range outside the range of applicability of the adiabatic approximation $\Omega \ll \gamma' \sim 10^7$ rad s^{-1}. The shift of the reference resonance with a change in Ω becomes nonmonotonic, reaching a maximum value at the higher Rabi frequencies, the higher the temperature of the active medium (Fig. 6b). At a certain temperature and sufficiently low Ω, an additional dip appears in the reference resonance, associated with a relatively strong absorption of fields with lower amplitudes, which makes it difficult to determine the magnitude of the shift S. In this regard, in Fig. 6b, the curves for temperatures of 60 and 55 °C are interrupted at those values of Ω at which a side minimum begins to appear.

Figure 7 shows how the resonance shape changes with an increase in the duration of the dark pause. The widths and

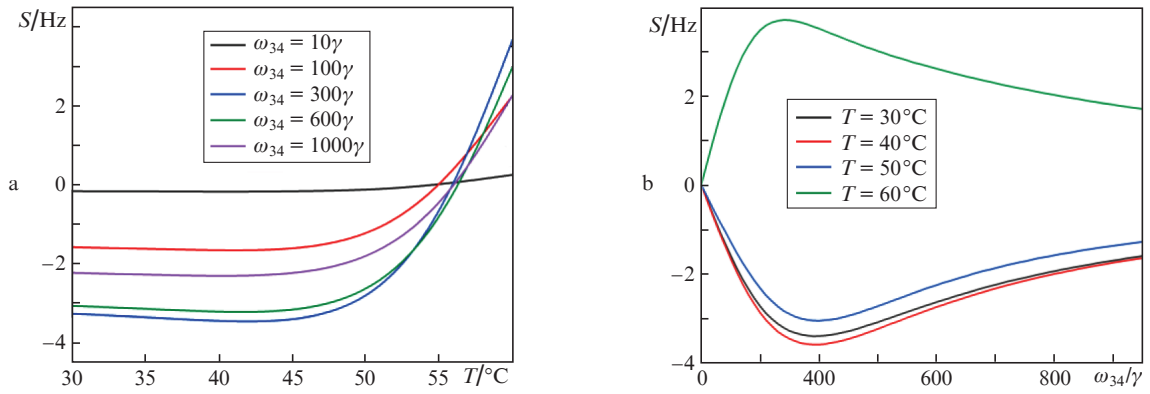

Figure 4. (Colour online) Dependences of (a) the reference resonance shift on the temperature at different ω_{34} and (b) the reference resonance shift on ω_{34} at different temperatures; the cell length $L = 1$ cm; other parameters are the same as in Fig. 2.

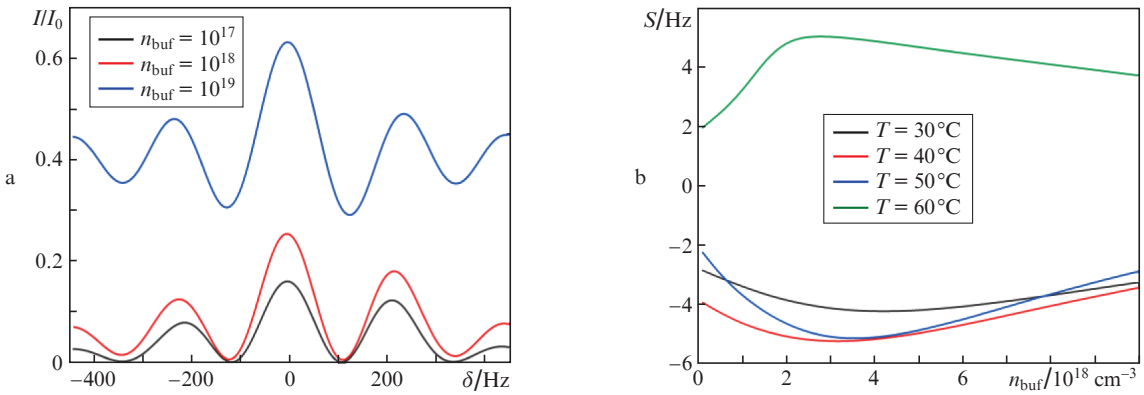

Figure 5. (Colour online) (a) Shapes of CPT resonances, detected by the Ramsey method from the intensity of the output radiation, for various buffer gas concentrations n_{buf} at a temperature $T = 45$ °C, as well as (b) dependences of the shift of the reference resonance on n_{buf} at different temperatures; $\omega_{34} = 300\gamma$, the cell length $L = 1$ cm, other parameters are the same as in Fig. 2.

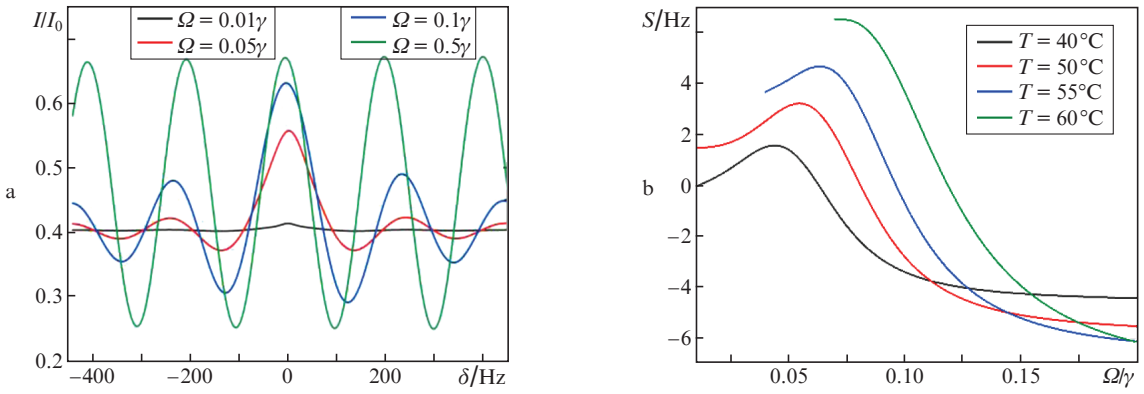

Figure 6. (Colour online) (a) Shapes of CPT resonances, detected by the Ramsey method from the intensity of the output radiation, for different Rabi frequencies $\Omega = \Omega_1 = \Omega_2$ common for both fields at a temperature $T = 45$ °C, as well as (b) dependences of the shift of the reference resonance on Ω at different temperatures; $\omega_{34} = 300\gamma$, the cell length $L = 1$ cm, other parameters are the same as in Fig. 2.

amplitudes of resonances decrease (Fig. 7a), and the shift behaves in a nonmonotonic manner (Fig. 7b). In particular, a change in the sign of the light shift is observed. In this case, the lowest sensitivity of the shift to temperature is achieved at $T_d \approx 1.2$ and 10 ms.

4. Conclusions

Based on the density matrix method in the Wigner representation, we have developed a consistent theory of interaction of bichromatic laser radiation with an optically dense medium

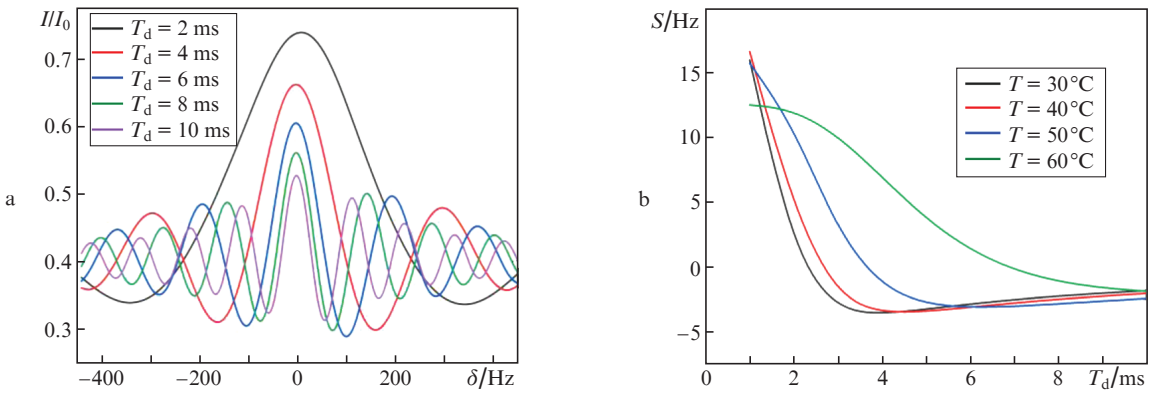

Figure 7. (Colour online) (a) Shapes of CPT resonances, detected by the Ramsey method from the intensity of the output radiation, for different times of the dark pause T_d at a temperature $T = 45$ °C, as well as (b) dependences of the shift of the reference resonance on T_d at different temperatures; the cell length $L = 1$ cm; other parameters are the same as in Fig. 2.

of alkali atoms having a nonzero temperature. The original system of integro-differential equations in partial derivatives has been reduced by a number of approximations to a system of ordinary differential equations of the first order. As a result of numerical modelling performed on the basis of this theory, resonances of coherent population trapping, detected by the Ramsey method, have been calculated. It has been shown that in an optically dense medium, the light shifts of the CPT resonance under pulsed pumping have a nontrivial dependence. The influence of the hyperfine splitting of the excited level, concentration of active atoms, temperature, and duration of the dark pause on light shifts has been analysed.

Acknowledgements. This work was supported by the RF President's Grants Council (Support to Young Candidates of Sciences Programme, Grant No. MK-1452.2020.2) and by the Russian Science Foundation (Grant No. 2172-10004, Development of numerical algorithms for solving systems of integro-differential equations). G.V. Voloshin acknowledges the support of the BASIS Foundation for the Advancement of Theoretical Physics and Mathematics in the studies of the peculiarities of the influence of the ensemble temperature and the associated motion of atoms on the collective effects caused by the finite optical thickness (Grant No. 21-1-1- 36-1).

References

1. Alzetta G. et al. *Nuovo Cimento B*, **36** (1), 5 (1976).
2. Arimondo E., Orriols G. *Lett. Nuovo Cimento*, **17** (10), 333 (1976).
3. Gray H.R., Whitley R.M., Stroud C.R. *J. Opt. Lett*., **3**, 218 (1978).
4. Agap'ev B.D., Gornyi M.B., Matisov B.G., Rozhdestvenskii Yu.V. *Phys. Usp*., **36** (9), 763 (1993) [*Usp. Fiz. Nauk*, **163** (9), 1 (1993)].
5. Akulshin A., Celikov A., Velichansky V. *Opt.Commun*., **84**, 139 (1991).
6. Schwindt P.D.D., Knappe S., Shah V., Hollberg L., Kitching J. *Appl. Phys. Lett*., **85**, 6409 (2004).
7. Andryushkov V., Radnatarov D., Kobtsev S., Dambuev A. *Proc. SPIE*, **11507** (1–6) (2021).
8. Harris S. *Phys. Rev. Lett*., **62**, 1022 (1989).
9. Kocharovskaya O.A., Khanin Ya.I. *JETP Lett*., **48**, 630 (1988) [*Pis'ma Zh. Eksp. Teor. Fiz*., **48**, 581 (1988)].
10. Peter D., Schwindt D., et al. *Appl. Phys. Lett*., **85**, 6409 (2004).
11. Yashuk V.V., Granwehr J., Kimbal D.F., et al. *Phys. Rev. Lett*., **93**, 160801 (2004).
12. Lukin M.D. *Rev. Mod. Phys*., **75**, 457 (2003).
13. Fleischhauer M., Imamoglu A., Marangos J.P. *Rev. Mod. Phys*., **77**, 633 (2005).
14. Zhang R., Wang X.-B. *Phys. Rev. A*, **94**, 063856 (2016).
15. Vanier J. *Appl. Phys. B*, **81**, 421 (2005).
16. Zibrov S.A., Velichansky V.L., Zibrov A.S., et al. *JETP Lett*., **82**, 477 (2005) [*Pis'ma Zh. Eksp. Teor. Fiz.*, **82**, 534 (2005)].
17. Kazakov G., Matisov B., Litvinov A., Mazets I. *J. Phys. B: At. Mol. Opt. Phys*., **40**, 3851 (2007).
18. Zibrov S.A., Novikova I., et al. *Phys. Rev. A*, **81**, 013833 (2010).
19. Barantsev K.A., Popov E.N., Litvinov A.N., Petrov V.M. *Radiotekh*., **12**, 164 (2016).
20. Khripunov S., Radnatarov D., Kobtsev S. *Proc. SPIE*, **9378**, 93780A (2015).
21. Kitching J. *Appl. Phys. Rev*., **5**, 031302 (2018).
22. Kobtsev S., Donchenko S., Khripunov S., Radnatarov D., Blinov I., Palchikov V. *Opt. Laser Technol*., **119**, 105634 (2019).
23. Ramsey N.F. *Phys. Rev*., **76**, 996 (1949).
24. Riehle F. *Frequency Standards: Basics and Applications* (Weinheim: Wiley-VCH Verlag GmbH, 2004; Moscow: Fizmatlit, 2009).
25. Zanon T., Guerandel S., de Clercq E., Holleville D., Dimarcq N., Clairon A. *Phys. Rev. Lett*., **94**, 193002 (2005).
26. Liu X., Mérolla J.M., Guerandel S., de Clercq E., Boudot R. *Opt. Express*, **21**, 12451 (2013).
27. Yano Y., Goka S., Kajita M. *Appl. Phys. Express*, **8**, 012801 (2014).
28. Yano Y., Goka S., Kajita M. *Appl. Phys. B*, **123**, 67 (2017).
29. Hafiz M.A., Coget G., Yun P., Guerandel S., de Clercq E., Boudot R. *J. Appl. Phys*., **121**, 104903 (2017).
30. Kobtsev S., Radnatarov D., Khripunov S., Popkov I., Andryushkov V., Steshchenko T. *J. Opt. Soc. Am. B*, **36**, 2700 (2019).
31. Kuchina E.A., Mikhailov E.E., Novikova I. *J. Opt. Soc. Am. B*, **33**, 610 (2016).
32. Boudot R., Maurice V., Gorecki C., de Clercq E. *J. Opt. Soc. Am., B*, **35**, 1004 (2018).
33. Baryshev V.N., Aleinikov M.S., Osipenko G.V., Blinov I.Yu. *Quantum Electron*., **48**, 443 (2018) [*Kvantovaya Elektron*., **48**, 443 (2018)].
34. Baryshev V.N., Osipenko G.V., Aleinikov M.S., Blinov I.Yu., *Quantum Electron*., **49**, 283 (2018) [*Kvantovaya Elektron*., **49**, 283 (2018)].
35. Barantsev K.A., Popov E.N., Litvinov A.N. *Quantum Electron*., **7**, 615 (2018) [*Kvantovaya Elektron*., **7**, 615 (2018)].
36. Hafiz M.A., Coget G., Petersen M., Calosso C.E., Guérandel S., de Clercq E., Boudot R. *Appl. Phys. Lett*., **112**, 244102 (2018).
37. Hafiz M.A., Coget G., Petersen M., Rocher C., Guérandel S., Zanon-Willette T., et al. *Phys. Rev. Appl*., **9**, 064002 (2018).
38. Liu X., Zhao X., Xu Z., Hu Z. *J. Opt. Soc. Am. B*, **38**, 1270 (2021).
39. Lenci L., Marmugi L., Renzoni F., et al. *J. Phys. B: At. Mol. Opt. Phys*., **52**, 085002 (2019).
40. Liu X., Lv Y.-N., Kang S., et al. *Opt. Express*, **29**, 2466 (2021).
41. Yudin V.I., Taichenachev A.V., Basalaev M.Yu., Zanon-Willette T., Pollock J.W., Shuker M., et al. *Phys. Rev. Appl*., **9**, 054034 (2018).
42. Yudin V.I., Taichenachev A.V., Basalaev M.Yu., Mehlstäubler T.E., Boudot R., Zanon-Willette T., et al. *New J. Phys*., **20**, 123016 (2018).
43. Basalaev M.Yu., Yudin V.I., Kovalenko D.V., Zanon-Willette T., Taichenachev A.V. *Phys. Rev. A*, **102**, 013511 (2020).
44. Kovalenko D.V., Basalaev M.Yu., Yudin V.I., Zanon-Willette T., Taichenachev A.V. *Quantum Electron*., **51** (6), 495 (2021) [*Kvantovaya Elektron*., **51** (6), 495 (2021)].
45. Barantsev K., Litvinov A. *J. Opt. Soc. Am. B*, **39**, 230 (2022).
46. Shuker M., Pollock J.W., Boudot R., Yudin V.I., Taichenachev A.V., Kitching J., Donley E.A. *Phys. Rev. Lett*., **122**, 113601 (2019).
47. Shuker M., Pollock J.W., Boudot R., Yudin V.I., Taichenachev A.V., Kitching J., Donley E.A. *Appl. Phys. Lett*., **114**, 141106 (2019).
48. Micalizio S., Godone A. *Phys. Rev. A*, **99**, 043425 (2019).
49. Voloshin G.V., Barantsev K.A., Popov E.N., Litvinov A.N. *J. Exp. Theor. Phys*., **156** (1), 1 (2020) [*Zh. Eksp. Teor. Fiz*., **156** (1), 5 (2019)].
50. Voloshin G.V., Barantsev K.A., Litvinov A.N. *Quantum Electron.*, **50**, 1023 (2020) [*Kvantovaya Elektron*., **50**, 1023 (2020)].
51. Rautian S.G., Smirnov G.I., Shalagin A.M. *Nelineinye rezonansy v spektrakh atomov i molekul* (Nonlinear Resonances in Spectra of Atoms and Molecules) (Novosibirsk: Nauka, 1979).
52. Taichenachev A.V., Yudin V.I., Wynands R., Stahler M., Kitching J., Hollberg L. *Phys. Rev. A*, **67**, 033810 (2003).
53. Taichenachev A.V., Yudin V.I., Velichansky V.L., Zibrov A.S., Zibrov S.A. *Phys. Rev. A*, **73**, 013812 (2006).
54. Kupriyanov D.V., Sokolov I.M., Havey M.D. *Opt. Commun*., **243**, 165 (2004).
55. Datsyuk V.M., Sokolov I.M., Kupriyanov D.V., Havey M.D. *Phys. Rev. A*, **77**, 033823 (2008).
56. Litvinov A.N., Sokolov I.M. *JETP Lett*., **113**, 763 (2021) [*Pis'ma Zh. Eksp. Teor. Fiz*., **113**, 791 (2021)].
57. Sokolov I.M., Kupriyanov D.V., Havey M.D. *J. Exp. Theor. Phys*., **122**, 246 (2011) [*Zh. Eksp. Teor, Fiz*., **139**, 288 (2011)].
58. Fofanov Ya.A., Kuraptsev A.S., Sokolov I.M., Havey M.D. *Phys. Rev. A*, **84**, 053811 (2011).
59. Javanainen J., Ruostekoski J., Li Y., Yoo S.-M. *Phys. Rev. Lett*., **112**, 113603 (2014).
60. Weiss P., Cipris A., Aráujo M.O., Kaiser R., Guerin W. *Phys. Rev. A*, **100**, 033833 (2019).
61. Kuraptsev A.S., Sokolov I.M. *Phys. Rev. A*, **101**, 033602 (2020).
62. Barantsev K., Kuraptsev A., Litvinov A. *Springer Proc. Phys*., **255**, 739 (2021).
63. Steck Daniel A. http://steck.us/alkalidata (2019).
64. Sheremet A.S., Gerasimov L.V., Sokolov I.M., Kupriyanov D.V., Mishina O.S., Giacobino E., Laurat J. *Phys. Rev. A*, **82**, 033838 (2010).
65. Barantsev K.A., Bozhokin S.V., Kuraptsev A.S., Litvinov A.N., Sokolov I.M. *J. Opt. Soc. Am. B*, **38**, 1613 (2021).